The Structure of Ribosome Inactivating Proteins

Jon D. Robertus* and Arthur F. Monzingo

Institute of Cellular and Molecular Biology, Department of Chemistry and Biochemistry, 1 University Station A5300, University of Texas, Austin TX, 78712, USA

Abstract: Ribosome Inactivating Proteins, RIPs, depurinate an invariant adenine from the 28S rRNA of eukaryotic ribosomes; they have evolved to near enzymatic perfection for this task. The N-glycosidase fold is conserved in plant and bacterial enzymes. RIPs can form complexes with cell surface recognition proteins that dramatically increase the cytotoxicity of the molecule.

INTRODUCTION

A number of organisms contain enzymes that can inhibit protein synthesis at a variety of points along that pathway. For example, the famous diphtheria toxin produced by *Corynebacterium diphtheriae* transfers the ADP-ribose group from NAD+ into the active site of eukaryotic translocation factor eEF2, and inhibits it [1]. This action kills the eukaryotic host cell and it is believed to thereby release iron required by the bacteria. Consistent with this hypothesis is the observation that the toxin promoter is controlled by iron [2].

An even more widespread enzyme activity is catalyzed by enzymes referred to as ribosome inactivating proteins, or RIPs. RIPs have been isolated primarily from higher plants, but they also occur in certain bacteria strains, like *Shigella dysenteriae*, and pathogenic strains of *Escherichia coli*, like the famous O57:H7 strain. RIP structure, function, and cytotoxicity have been reviewed extensively. Some important and/or recent reviews include: [3 - 7].

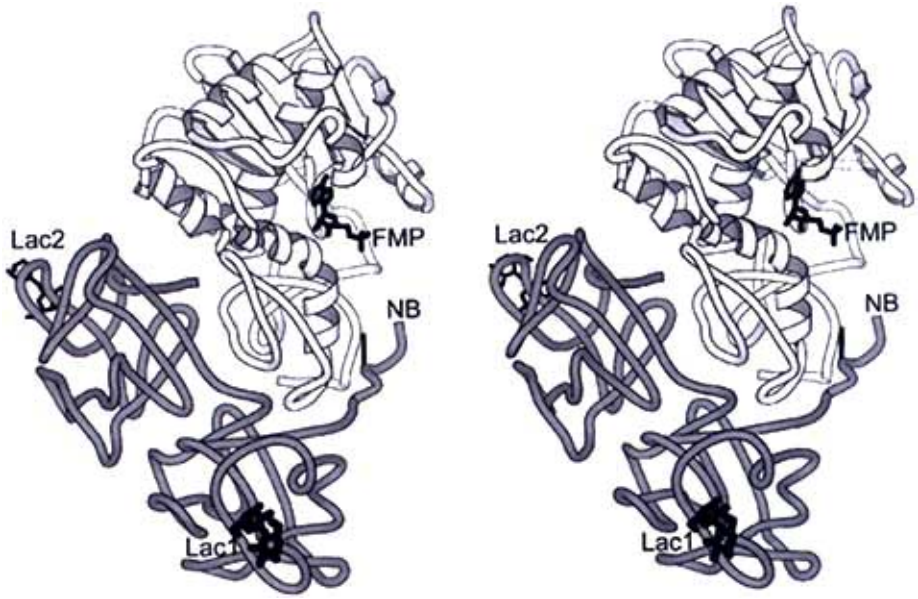

Fig. (1). Ribbon representation of ricin. The A chain, RTA, is shaded light in the upper right, and the B chain, RTB, is shaded dark in the lower left. Several ligands are shown in thick black bonds. The active site of RTA contains the substrate analog FMP. RTB is formed from two similar domains each with a galactose binding site. Those sites are shown occupied by the disaccharide lactose; Lac1 is in the N-terminal domain and Lac2 is in the C-terminal domain. RTA and RTB are linked by a disulfide bond between Cys 259 of RTA and Cys 4 of RTB; this is indicated as a short line near the RTB N-terminus that is labeled NB.

It is now known that RIPs are RNA N-glycosidases; they have evolved to depurinate a key adenine base in an invariant site on the ribosomal 28 S rRNA [8,9]. This depurination prevents elongation factors from binding properly to the ribosome and the inhibition of protein synthesis is generally lethal to the cell. The k_{cat} for the depurination of ribosomes is on the order of 1000/sec and the K_m for ribosomes is of the order of 0.1 μM [10 - 12]. It should be noted that the specificity constant, k_{cat}/K_m, for these enzymes approaches

*Address correspondence to this author at the Institute of Cellular and Molecular Biology, Department of Chemistry and Biochemistry, 1 University Station A5300, University of Texas, Austin TX, 78712, USA; E-mail: jrobertus@mail.utexas.edu

1389-5575/04 $45.00+.00

the diffusion limit of the ribosomal substrate, suggesting that the N-glycosidase mechanism has evolved to near enzymatic perfection.

RIPs fall into two broad structural classes. Type-1 RIPs are single chain proteins of Mr ≈ 30,000. Examples include PAP, trichosanthin, gelonin, and many others [13]. It appears that these proteins have evolved to protect the host plant from pathogens. PAP, for example, is localized in the cell wall space, and enters the cytoplasm when the wall is breached, inhibiting the translation machinery and retarding viral replication [14]. It has also been shown that expression of PAP in transgenic tobacco plants increases resistance to certain viruses [15].

Type-2 RIPs combine an N-glycosidase A chain with a cell surface binding chain, or chains. In most type-2 RIPs from higher plants, the A chain is combined with a single B chain. Examples of type-2 RIPs include ricin, abrin, modeccin, and ebulin. Type-2 bacterial toxins, like Shiga toxin, combine a single N-glycosidase A chain with five smaller B chains. It is generally assumed that type-2 plant RIPs serve as defensive agents, but instead of being rather passive these proteins assume the best defense is a good offense. The heterodimeric RIPs are often found in seeds, where they act as powerful cytotoxins to any animal that consumes them. Type-2 RIPs in leaf tissue may also protect against insects. The B chains of type-2 RIPs bind strongly to the cell surfaces of the predator, effectively increasing the toxin concentration and facilitating internalization of the A chain. Once in the cytoplasm, the A chain inhibits protein synthesis in the same way as the type-1 RIPs. The B chains render type-2 RIPs far more cytotoxic than type-1 enzymes. For example, ricin has an intravenous LD_{50} of <3 μg/Kg body weight for mice [16], and rabbits may be 10 times more susceptible [3]. Tests against cultured cells suggest type-2 RIPs are roughly 10^5 times more cytotoxic than type-1 RIPs [17].

THE STRUCTURE OF RICIN

Ricin is the archetypal, most thoroughly studied, of all RIP enzymes, and it was the first for which an X-ray structure was available [18]. That structure was refined at 2.5 Å resolution [19], and the A chain (RTA) and B chain (RTB) structures were described in detail [20, 21]. Subsequently, the recombinant A chain, expressed in bacteria, was refined at 2.3 Å [22] and independently at 1.8 Å resolution [23]. (Figure. **1**) shows a representation of the heterodimeric ricin toxin.

RTA is a globular enzyme of 267 amino acids, with a number of secondary structural elements; these are listed in (Table. **1**). The fold, and catalytic mechanism, of RTA is maintained in all other RIP N-glycosidases. As a consequence, a description of RTA largely defines the A chain of other type-2 RIPs and also the type-1 RIPs.

Table. 1. Secondary Structure Elements of RTA

α-Helix	Residues	β Strand	Residues
A	18 - 32	a	7 - 13
B	99 - 104	b	56 - 64
C	122 - 127	c	68 - 76
D	141 - 152	d	79 - 86
E	161 - 180	e	88 - 93
F	184 - 192	f	113 - 117
G	202 - 210	g	230 - 234
H	211 - 219	h	237 - 242

RTA has a pronounced active site cleft able to recognize and accommodate the rRNA stem-loop which is its target. This cleft was initially mapped by binding formycin monophosphate (FMP), a non-hydrolysable analog of the normal adenine substrate, into the ricin crystals [24]. The orientation of FMP in the active site is shown in (Figure. **2**). It shows that the adenine ring binds between two Tyr residues, 80 and 123 in RTA, that are invariant in the RIP family. The structure also suggested that Glu 177 and Arg 180, also invariant residues, might be important in the N-glycosidase mechanism. That same study also revealed the structure of the complex with the dinucleotide ApG, where the adenine moiety bound into the specificity pocket in essentially the same manner as formycin.

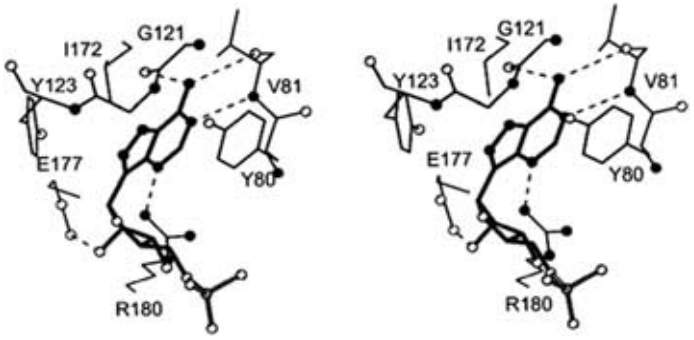

Fig. (2). Binding of FMP to the RTA active site. The substrate analog FMP is shown in thick bonds, while the protein groups are thinner. Oxygen atoms are shown as open circles and nitrogens as solid circles. Hydrogen bonds are shown as dashed lines.

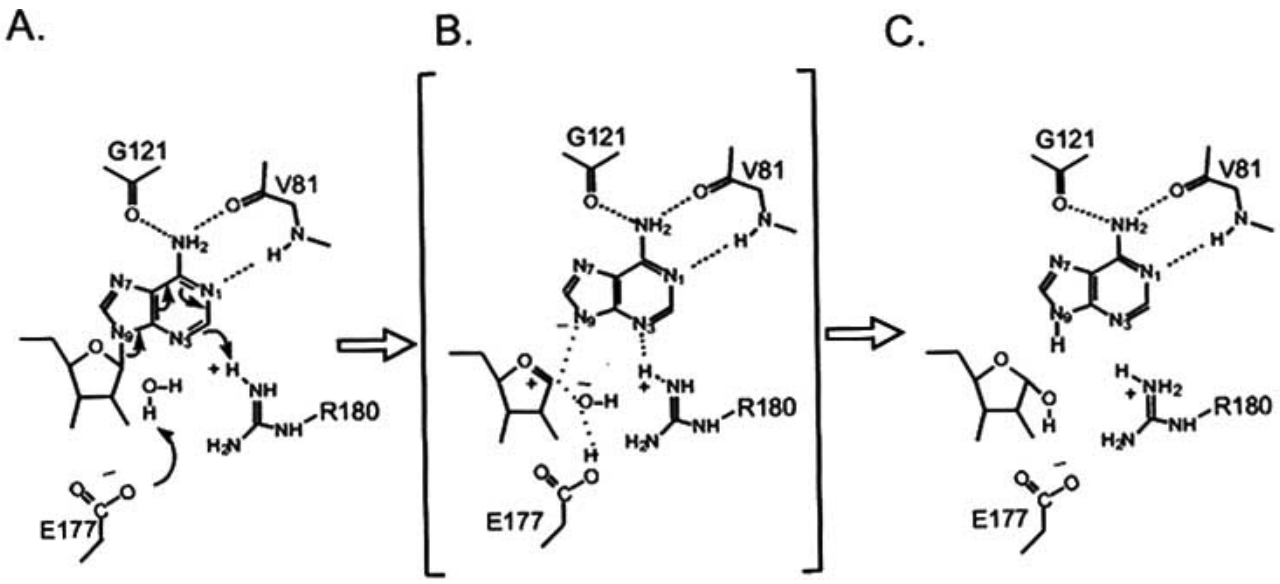

Fig. (3). A plausible mechanism for ricin and the RIP family. The susceptible adenine binds in a specificity pocket and contacts the side chain of two invariant tyrosines that are not shown in the figure. Y80 lies above the adenine and is stacked on it, while Y123 lies below. A possible transition state structure is indicated in brackets as panel B. C1'-N9 bond breaking is catalyzed and the polarization is aided by partial, or possibly complete, protonation of N3 by Arg 180. The putative transition state, panel B, shows negative charge developing on the leaving adenine and positive charge on the ribose in the form of an oxocarbenium cation. Water is the ultimate nucleophile and in this figure it is shown being polarized by the basic side chain of E177. Alternatively, the E177 carboxylate may serve to stabilize the oxocarbenium ion.

The X-ray structure was used to guide a series of site-directed mutation experiments that proved the importance of all these groups [25, 26, 27, 12]. In particular, it was shown that conversion of Arg 180 to Gln (R180Q) reduced activity 2500 fold and conversion of Glu 177 to Gln (E177Q) reduced activity at least 170 fold. These residues figure prominently in the mechanism of action for N-glycosidation, which is thought to proceed by partial protonation of the leaving adenine at N3 by Arg 180, while Glu 177 serves as a general base to polarize the attacking water molecule.

A plausible mechanism for ricin, and the entire class of RIPs is shown in (Figure. **3**). As the C1'-N9 bond breaks negative charge accumulates in the adenine ring and positive charge in the ribose ring. The former is stabilized by partial, or complete, protonation of N3 by Arg 180. This purely structural finding was surprising since acid/base depurination in organic media is thought to proceed by protonation at N7. However, elegant mechanistic studies by Schramm and his coworkers confirmed that ricin depurination does not involve N7 protonation [28]. Those studies also showed that the

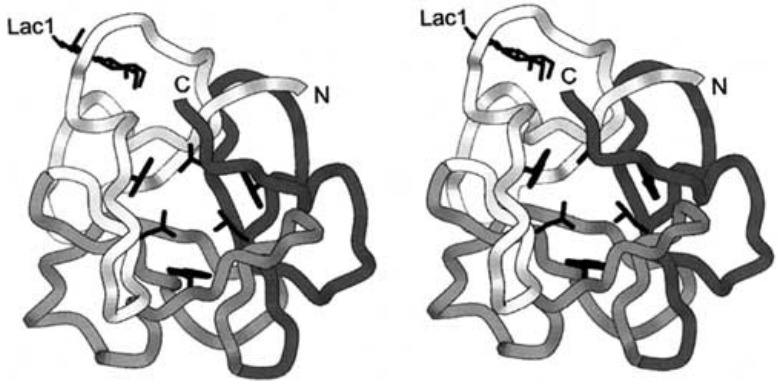

Fig. (4). The N-terminal domain of RTB. RTB is the product of an elaborate evolutionary history in which three galactose binding units were fused to make a domain and then two domains fused to make modern RTB. The 3-fold pseudo symmetry is evident in this ribbon drawing of domain 1 of RTB, where each subdomain is shaded differently. Each contributes hydrophobic residues to the central core; a set of three tryptophans, edge on, and three aliphatic residues are shown as black bonded groups in the center. Of the three potential galactose binding sites, only site α retains sugar binding capacity; its position is marked by the galactose-containing disaccharide lactose labeled as Lac1.

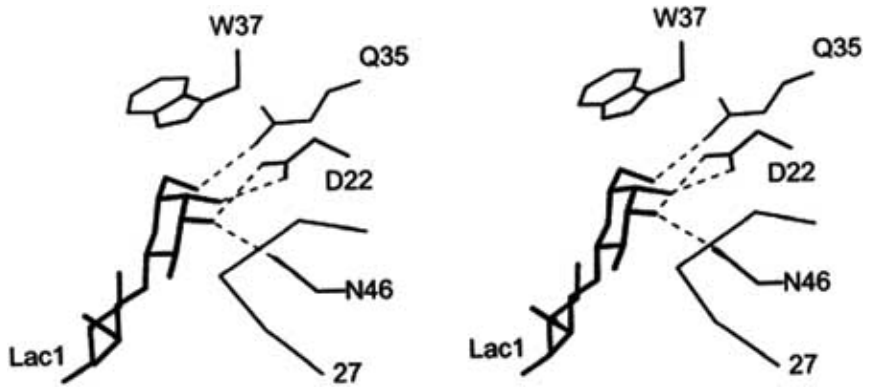

Fig. (5). Interactions of lactose with the N-terminal domain of RTB. A shallow cleft accommodates the galactose moiety of lactose (shown in thick black bonds). The RTB cleft is formed by the side chain of Trp 37 on the top, and a kinked segment of backbone, shown here from residues 23 to 27 and labeled at position 27. Specific hydrogen bonds, shown as dashed lines, are formed to the sugar from key, labeled, side chains.

ricin reaction transition state has oxocarbenium character on the ribose. This was further confirmed by the synthesis of novel compounds that incorporated the cationic character, as amines, into a ribose analog. As expected for true transition state analogs, these were potent, tightly binding, ricin inhibitors [29]. The exact role of the invariant Glu 177 is still unclear. It may act to polarize water, as suggested in (Figure. **3**), or it may simply pair with, and electrostatically stabilize, the transition state oxocarbenium.

As a type-2 RIP, ricin has a cell surface recognition chain, RTB. The X-ray analysis of ricin provided a fascinating insight into the evolution of the plant-derived B chains. As shown in (Figure. **1**), RTB is a dumbbell shaped protein with two domains; Domain 1 consists of residues 1 - 135, and domain 2 consists residues 136 - 262. What is not immediately apparent is that these domains are homologues [30] and that each of the domain is constructed from three homologous subdomains, called α,β, and γ, together with an unrelated linker, or α, unit [31]; (Figure. **4**) shows the pseudo-three-fold symmetry of the N-terminal domain of RTB. These subdomains are each approximately 40 residues in length. Although the α,β, and γ subdomains exhibit the same basic fold, only the 1α and 2γ units, on the extreme ends of the RTB dumbbell, retain the ability to bind galactosides. The details of the interactions between galactose and the α subdomain of the N-terminal domain of RTB are shown in (Figure. **5**). Conserved residues in

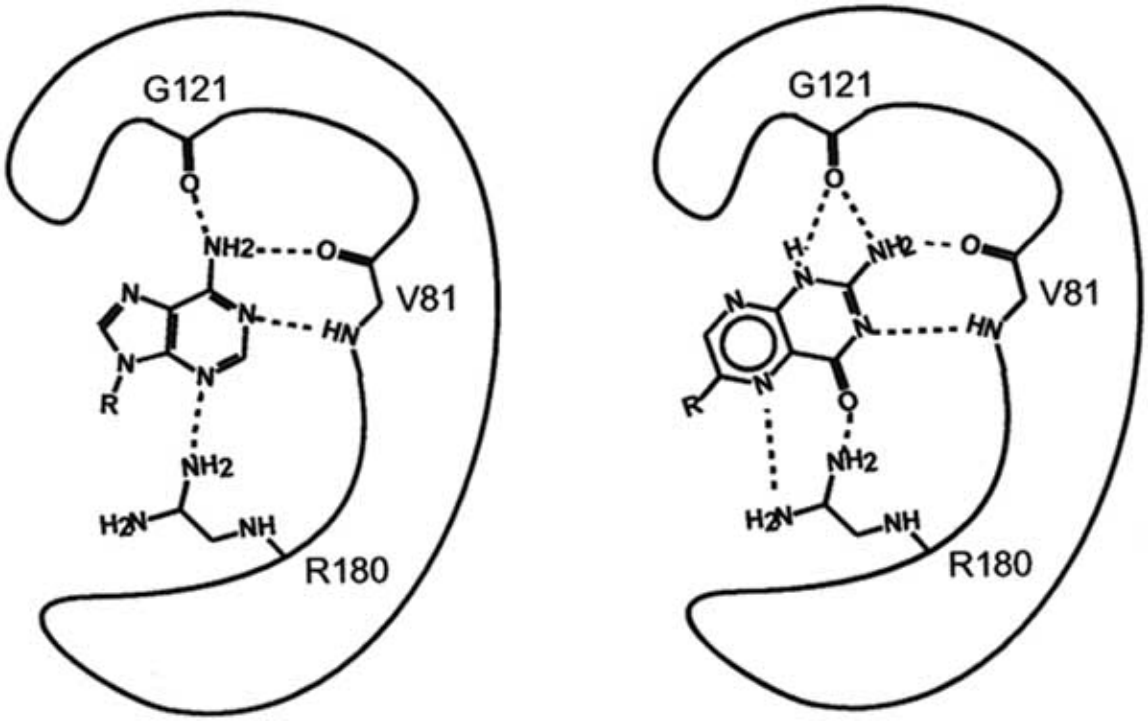

Fig. (6). Interactions of adenine and PTA with RTA. The panel on the left is a cartoon of the RTA active site and its hydrogen bond interactions with adenine. The Tyr 80 side chain lies above the plane of the adenine and is stacked on it. Tyr 123 interacts with the underside of adenine. The right panel shows the observed interactions of RTA and the inhibitor PTA. Note that more hydrogen bonds are made, and they tend to be shorter, that is stronger, than those to adenine.

subdomain γ of the C-terminal domain bind a second galactoside in a similar fashion.

RICIN INHIBITOR DESIGN

Ricin is a well-known cytotoxin, and it has a colorful history as a poison. It was used in the famous "umbrella tip" assassination of Georgi Markov by the KGB [32] and has been prepared by so-called "patriot" groups as an agent of domestic terrorism [33]. Ricin was used as a biological warfare agent by Iraq [34]. Documents captured by British commandos in Afghanistan in 2001 revealed that ricin had been adopted as a terrorist weapon by the al-Qaeda group [35]. Because of its ease of production and documented use as a biological weapon, there has been considerable interest in developing antidotes to ricin and related toxins.

The natural substrate for RTA is rRNA, and some ricin inhibitors have used RNA as an inhibitor platform. These include efforts to select for strongly binding RNA aptomers [36] and use of RNAs that incorporate putative catalytic transition state geometry [29]. However, due to poor bioavailability, uptake, and stability these RNA-based inhibitors are unlikely to be developed into useful antidotes; it is more likely that smaller organic inhibitors will fill this role.

The first RTA inhibitor identified was Pteroic Acid, PTA [37]. PTA was identified using a computer-based "virtual screen" in which some 250,000 compounds were tested for complementarity in shape and charge to the active site of RTA. PTA was tested kinetically to show it was indeed an inhibitor, and the X-ray structure of the complex was solved to confirm the binding mode. The structure of the complex revealed the inhibitor mimicked many attributes of the natural adenine substrate, but made more and stronger interactions with RTA. (Figure. **6**) is a cartoon representation comparing the observed binding of adenine and the pteroic acid moiety of PTA.

Since the discovery of PTA as an inhibitor, additional work on antidote design has been carried out. A computer-modeling method showed that additional platform molecules could serve as the basis for inhibitor design [38]. Some of these models were implemented in a systematic search for

Table. 2. RIP Structures

Protein	Species	Res. (Å)	PDB ID	Reference
Type-1				
pokeweed antiviral protein (PAP)	*Phytolacca americana*	2.50	1PAF	[44]
		2.10	1QCG	[47]
α-PAP	*Phytolacca americana*	2.30	1APA	[64]
*momordin I / α-momorcharin	*Momordica charantia*	2.16	1MOM	[51]
		2.00	1AHC	[45]
		2.20	1MRI	[46]
		2.20	1F8Q	[56]
†momordin II / β-momorcharin	*Momordica charantia*	2.55	1CF5	[57]
/ MAP30		-----	1D8V	[65]
α-trichosanthin	*Trichosanthes kirilowii*	1.88		[66]
		2.00		[48]
gelonin	*Gelonium multiflorum*	1.80		[52]
bryodin 1	*Bryonia dioica*	2.10	1BRY	[67]
saporin SO6	*Saponaria officinalis*	2.00	1QI7	[68]
Type-2				
ricin	*Ricinus communis*	2.50	2AAI	[19]
ricin (A chain)		2.30	1RTC	[22]
ricin (A chain)		1.80	1IFT	[23]
Shiga toxin	*Shigella dysenteriae*	2.50	1DM0	[41]
abrin-a	*Abrus precatorius*	2.14	1ABR	[53]
mistletoe lectin I	*Viscum album*	2.70	1CE7	[55]
ebulin 1	*Sambucus ebulus*	2.80	1HWM	[43]

*α-momorcharin is a synonym for momordin I

†β-momorcharin and MAP30 are synonyms for momordin II

optimized platforms. The compound 8-methyl-9-oxaguanine, designed and synthesized in this program, was found to be a water-soluble platform of reasonable potency [39]. The compound 4-aminopyrazolo[3,4-d]pyrimidine (4-APP) was also identified as a weak inhibitor of ricin and related RIPs [40]. To be truly effective antidote drugs, the specificity and bioavailability of RTA inhibitors needs to be substantially improved, and this is an ongoing interest in several laboratories.

THE STRUCTURE OF OTHER RIPS

To date, the structures of ten type-1 and five type-2 RIPs have been solved, one, MAP30, by NMR and all others by X-ray crystallography. These RIPs are listed in (Table. **2**). With the exception of the bacterial Shiga toxin, all of the RIPs whose structure has been determined have come from higher plants.

The structures of the type-1 RIPs and the A chains of the type-2 RIPs are very similar. When each is compared with ricin A chain, the rms distance between corresponding Cα positions is generally less than 2.0 Å. The only exceptions are saporin SO6 with an rms deviation of 2.2 Å and the A chain of Shiga toxin with an rms deviation of 2.8 Å. The similarities of these structures are shown in (Figure. **7**). In panel A, the A chain of ricin is superimposed with two type-1 RIPs. Momordin I, isolated from the bitter pear, is one of the first RIPs solved by X-ray diffraction; the rms deviation

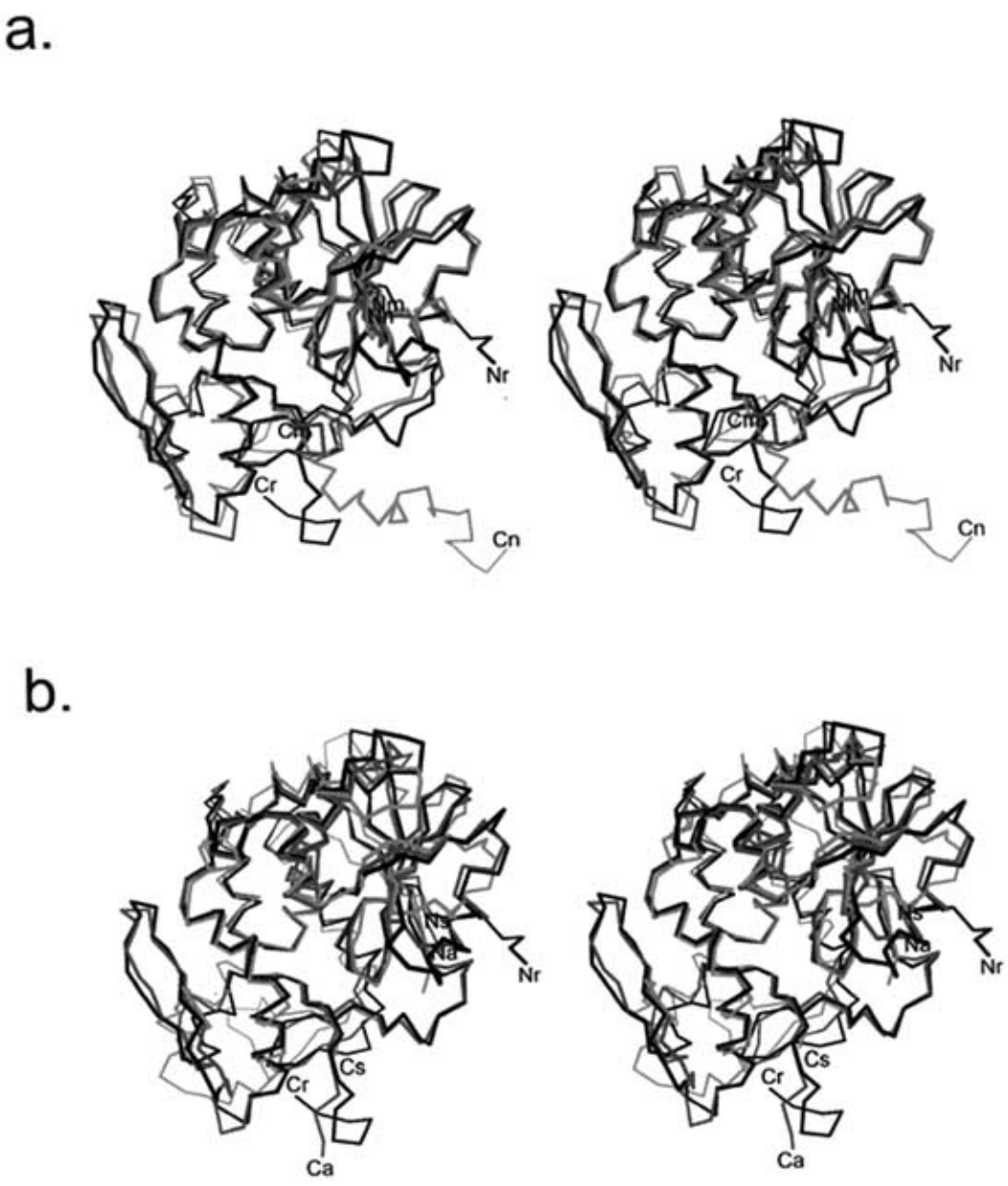

Fig. (7). Comparison of RIP backbones. The Cα carbons of various RIPs were aligned, in a least squares sense, with the backbone of ricin A chain. a) Type-1 RIPs aligned with ricin A. Ricin A is shown in black and its termini labeled Nr and Cr; momordin I is shown in the middle shade of gray with terminal labels Nm and Cm; MAP30, solved by NMR, is shown in light gray with termini labeled Nn and Cn. b) Type-2 RIP A chains. Ricin A is black and labeled as above; abrin A is in the middle shade, labeled Na and Ca, and the bacterial Shiga A chain is in light gray with termini labeled Ns and Cs.

of corresponding Cαs is 1.04 Å. MAP30 is a type-1 RIP solved by NMR with the consensus confirmation displayed; the rms deviation of corresponding Cαs is 1.47 Å. Notice that the labeled N and C termini of the RIPs differ in length. These short regions can assume different conformations, but the vast bulk of the protein folds are clearly very similar and the active site geometries are nearly identical.

In panel B, the ricin A chain is superimposed with two other type-2 A chains. Abrin is a typical type-2 RIP isolated from higher plants. Like ricin, it has been studied biochemically for many years. The rms deviation of corresponding Cαs between abrin and ricin A chains is 1.0 Å. Also shown is the superposition with the A chain from the bacterial Shiga toxin. As stated above, it has the largest deviation from RTA of any known RIP. As for the type-1 RIPs, the termini of the type-2 RIPs can vary in length and local conformation. The main body of the RIPs is very similar however, with one exception. Notice that there is also a significant difference between the Shiga A and the two plant RIPs in the hairpin loop on the extreme left of the molecules. This loop is involved in close contacts with the B chain of the plant RIPs. However, the bacterial Shiga toxin lacks a homologous B chain and instead contains a pentamer of 69 amino acid B chains that bind cell surface glycolipids [41]. It is this difference in A chain/B chain geometry that allows the loop region of the A chains to differ so markedly.

The structures of the B chains of the type-2 RIPs from plants are also quite similar. When compared with the ricin B chain, each has an rms distance between corresponding Cα positions of 1.3 Å or less. However, the galactose binding residues (see Figure. **5**) can vary between proteins. For example, the type-2 RIP called ebulin is 300 times less cytotoxic than ricin, although it's A chain has essentially the same enzymatic activity [42, 17]. This lack of cytotoxicity was traced to a reduced affinity for galactosides, principally in the 2γ of the ebulin B chain [43]. The amino acids of sugar binding site 1α are identical between the two proteins, but there is a replacement of ricin Tyr 248 in site 2γ by a Phe in ebulin B chain. There are also more subtle geometric rearrangements that make it difficult to bind an extended polysaccharide. The weakly toxic agglutinin called RCA is a ricin homologue with subunit composition A_2B_2. Each of the two B chains binds only a single galactoside. Site 1α is again, intact, but in site 2γ the key Tyr 248 has been converted to a charged histidine [21].

THE STRUCTURES OF RIP COMPLEXES

The structures of several complexes with compounds bound in the active site of RNA N-glycosidases (type-1 and the A chain of type-2 RIPs) have been determined and are listed in (Table. **3**). The compounds bound fall into 3 categories: adenine derivatives, pterin derivatives, and guanine derivatives.

As described earlier, the initial work of binding substrate analogs to RIPs was done with the ricin A chain and FMP [24], as shown in Fig. (**2**). Subsequent experiments with RIPs and both FMP and formycin have shown essentially the same mode of binding [23, 44 – 46].

The binding of the adenine ring of adenosyl(3'->5')guanosine (ApG) was found to be very similar to that of the formycin ring of FMP [24]. In determining this structure, good electron density was observed for the adenosine moiety of the dinucleotide, but only weak density was seen for the guanosine moiety, indicating that guanine was not being tightly bound in a specific receptor site. A subsequent study binding ApG to PAP again showed strong density for the adenine ring and only part of the adjoining ribose but only very diffuse density for the guanosine moiety [47].

Only the product adenine was found bound when crystals of α-trichosanthin were soaked with ApG [48], raising a question about hydrolytic activity in the crystals. As shown in (Table **3**), several other adenine-containing compounds have been bound to RIPs with only the adenine ring being observed, suggesting that hydrolysis of the N-glycosidic bond is indeed occurring. In general, these compounds are not substrates for RIPs in steady state kinetic studies, but with high concentrations (> 1 mM) and long soaking times (several hours and even much longer), there appears to be some catalytic turnover with retention of only the leaving adenine group in the active site cleft. In all of these experiments, the adenine ring was found to bind in a manner similar to what had been originally observed with FMP. In contrast to other adenine derivatives, NADPH was found bound intact to α-trichosanthin [49].

A virtual screen for RIP inhibitors identified pteroic acid (PTA), and kinetic and crystallographic analysis showed this was true [37]; its binding is represented in Fig. (**6**). The electron density for the pterin ring clearly indicates the disposition of the exocyclic amine and oxo groups and allows for an unambiguous orientation of the group. A similar mode of binding was observed in the ebulin-PTA complex [43], but a different mode of binding has been reported for PTA complexed with PAP [47]. In this report, the pterin ring is proposed to be flipped 180° from the orientation observed with RTA and ebulin, although both orientations fit the electron density.

Additional platform molecules, such as guanine, have been identified as the basis for further inhibitor design [38]. The structures of RTA complexed with 8-methyl-9-oxaguanine and other inhibitors designed from the guanine platform have been solved [39]. The observed binding of these molecules differs from that expected based on the binding of adenine and PTA as well as that observed with guanine bound to PAP [50].

In these active site complexes, the position and orientation of most active site residues remains fixed in the various RIPs. However, some variability has been observed in the orientation of an invariant active site tyrosine residue (80 in ricin A) among RIPs, both in the ligand bound and unbound states. This observation has led to speculation that this conformational movement may play a role in catalysis [45, 48, 51-53]. In the native ricin, the side chain of Tyr 80 is oriented so that it can hydrogen bond to the peptide oxygen of residue 121, across the active site [20]. Upon the binding of the substrate, there is slight movement of the main chain and rotation of Tyr 80 about the Cα-Cβ bond, breaking the hydrogen bond with Gly 121 and allowing for

Table. 3. Ligands Observed Bound to RIP N-Glycosidases

Ligand Bound	Ligand Observed	Protein	Res. (Å)	PDB ID	Reference
FMP		ricin	2.80	1FMP	[24]
FMP		PAP	2.80	1PAG	[44]
FMP		α-momorcharin	2.20	1AHB	[45]
formycin		ricin (A chain)	2.40	1IFU	[23]
formycin		α–momorcharin	2.00	1MRH	[46]
formycin		α-trichosanthin	1.60	1MRK	[46]
ApG		ricin	3.00	1APG	[24]
ApG	adenine	PAP	2.00	1QCI	[47]
ApG	adenine	α-trichosanthin	1.86	1QD2	[48]
AMP	adenine	ricin (A chain)	2.00	1IFS	[23]
adenosine	adenine	α-momorcharin	2.20	1AHA	[45]
ATP	adenine	α–momorcharin	1.80	1MRG	[46]
ATP	adenine	α-trichosanthin	1.60	1MRJ	[46]
GpA	adenine	α-trichosanthin	1.89		[48]
NADH	adenine	α-trichosanthin	1.93		[48]
2',5'-ADP	adenine	α-trichosanthin	1.90		[48]
ApCpC	adenine	PAP	2.10		[47]
NADPH		α-trichosanthin	1.70	1TCS	[49]
AMP		ricin (A chain) (R180H mutant)	2.80	1OBT	[54]
neopterin		ricin (A chain)	2.50	1BR5	[37]
pteroic acid		ricin (A chain)	2.30	1BR6	[37]
pteroic acid		PAP	2.10	1QCJ	[47]
pteroic acid		ebulin	3.10	1HWP	[43]
guanine		PAP	2.10	1D6A	[50]
7-deazaguanine		ricin (A chain)	2.80	1IL3	[39]
9-deazaguanine		ricin (A chain)	2.60	1IL4	[39]
2,5-diamino-4,6-dihydroxypyrimidine		ricin (A chain)	2.80	1IL5	[39]
8-methyl-9- oxoguanine		ricin (A chain)	3.10	1IL9	[39]

the insertion of the adenine ring into the active site [24]. When AMP was bound to the R180H mutant of RTA in an apparently unproductive mode, this hydrogen bond was not broken, possibly due to a strong interaction between Tyr 80 and the mutant His 180 [54]. The hydrogen bond between Tyr 80 and residue 121 has not been observed with equivalent residues in other RIPs, where the movement of the tyrosine residue only involves rotation about the Cα-Cβ bond. The orientation of the tyrosine residue differs among native RIPs; and for a given RIP, binding of a substrate analog may result in the rotation of the tyrosine. However, there is no consistent pattern of conformational change of the tyrosine among RIPs. The flexibility of this residue may facilitate substrate binding, but the residue does not directly participate in the hydrolytic reaction.

RIPS AS GLYCOPROTEINS

The plant RIPs are frequently expressed as glycoproteins. Oligosaccharides covalently bound to the side chain of asparagine residues have been modeled with the structures of the B chains of three type-2 RIPs: ricin [21], abrin-a [53], and mistletoe lectin I [55]. Ricin A chain is also known to be glycosylated; but no oligosaccharides were seen bound to

the A chain in the ricin crystal structure probably because non-glycosylated molecules were selected in crystal formation [20]. Oligosaccharide has been modeled covalently bound to the A chain of mistletoe lectin I [55] and to several type-1 RIPs: gelonin [52], α-momorcharin [56], and β-momorcharin [57]. Glycosylation is clearly not necessary for the activity of ricin A chain (and other RIPs, by inference) as demonstrated with recombinant RTA [12].

PUTATIVE NON-RIP ACTIVITIES OF RIPS

There have been claims that in addition to the exquisitely specific depurination of ribosomal RNA, RIPs also catalyze related reactions, such as DNA hydrolysis, or depurination of other RNAs. These studies tend to be phenomenological, using gels to show that some nucleic acid has been modified at a very slow rate, and rarely examine the putative reaction in an explicitly quantitative way. In particular, no complexes between these substrates and an RIP have been seen at high resolution and so structural interpretations must be guarded.

It has now been shown unequivocally that the weak "DNase" activity reported for several RIPs was in fact due to trace contamination by nucleases [58]. When RIPs like ricin and PAP were expressed from cloned genes in *E. coli*, the purified RIPs lacked the contaminating enzymes so common in plants, and no DNA hydrolysis was observed. (This is confirmed by unpublished experiments in our laboratory). Furthermore, Day *et al.* went on to isolate the contaminating nucleases from plant sources and showed that all of the putative DNase action ascribed to the RIP was in fact due to these contaminants.

There is no definitive study showing that hydrolysis of non-ribosomal RNAs by RIP-containing solutions is due to contamination, but the enzymatic efficiency of these reactions is poor. It is instructive to examine some of these studies quantitatively to try to assess their importance. For example, one study reported that PAP could release adenine from HIV RNA [59]. However, in that study 250 pmoles of RIP released only 168 pmoles of adenine in an hour - a rate 30,000 to 100,000 times slower than the rate of specific adenine release from ribosomes. In a similar vein it was reported that 250 pmoles of PAP could release 143 pmoles of guanine from *E. coli* rRNA in 4 hours [60], a rate, again, on the order of 10^5 times lower than the natural depurination of the specific ribosomal adenine target.

Schramm and co-workers carried out a thorough and systematic analysis of ricin depurination of naked RNA oligomers. They found that RTA depurinates a single adenine from an optimized synthetic RNA stem-loop structure at a rate of 219/minute. This activity has an optimum pH near 4.0 and is controlled by a group with a pKa near 4.5 [28]. As a consequence, activity at physiological pH would be expected to be roughly 1000 times slower and in fact depurination occurs at a barely detectable rate at neutral pH. (Depurination of naked DNA by momordin II has also been demonstrated at pH 4.0 [69]). At this time we cannot use the structure of ricin or other RIPs to rationalize this pH effect. It is not clear if the controlling residue is on the enzyme or on the substrate. Glu 177 is known to be a key catalytic residue for ricin, and Glu 208 is also near the active site cleft. It is unclear why deprotonation of either residue would be essential to attacking naked nucleic acids, but not those in intact ribosomes. The requirement of unnaturally acid pH to depurinate naked nucleic acids at a measurable rate suggests this is a side reaction that has little relevance in a cellular environment.

To put such phenomenon in perspective, it should be noted that many enzymes catalyze side reactions at a very low rate. Chymotrypsin is well-known to hydrolyze peptide bonds in which the carbonyl group is donated by aromatic residues, but it can also cleave at other residues, even lysine which is normally attacked by trypsin not chymotrypsin. As noted in a review of chymotryptic digestion, "but cleavage at these sites is usually significant only at a high concentration of enzyme or when prolonged digestion is employed" [61]. Another example of how failure to attend to relative kinetic parameters can lead to misunderstanding is seen in the analysis of EPSP synthase, an enzyme in the shikimic acid synthetic pathway. The mechanism and rates for that enzyme had been well established by Anderson and Johnson, when another group detected a "novel" intermediate [62]. It was subsequently shown, however, that this new intermediate was in fact a side product that formed at a rate roughly one million times slower than the real reaction and could only be seen on time scales that were unreasonably long. In reviewing the errant paper it was stated, "the confusion and the errors that can result when the rate of formation of a compound is overlooked are illustrated in (this) paper" [63].

It seems likely that the unusual RIP reactions are, at best, side reactions on the near perfect RIP depurination of ribosomes. They probably occur when a nucleic acid substrate is forced into the RIP binding cleft, where upon a version of the hydrolytic reaction can occur at a very poor rate. This extremely poor reactivity does not preclude the possibility that these side reactions might be of practical value in certain specialized cases.

In conclusion, it seems prudent to be very cautious in interpreting non-RIP phenomenon as a major role for these enzymes, especially since the rates observed are so low that it is always difficult to rule out inadvertent action by a trace contaminating enzyme. It is clear that ricin and other RIPs have evolved to enzymatic perfection at the task of depurinating one particular adenine, at physiologic pH, in the context of an intact ribosome.

ACKNOWLEDGEMENTS

This work was supported by grants GM 30048 from the National Institutes of Health, and by grants from the Foundation for Research and the Welch Foundation, and by the College of Natural Sciences support to the Center for Structural Biology.

REFERENCES

[1] Eisenberg, D.; Bell, C.E.; Bennett, M.J.; Collier, R.J.; Schlunegger, M.P.; Steere, B.A.; Weiss, M.S. in *Protein Toxin Structure*; Parker, M. W., Ed.; Landes: Austin, TX, **1996**; pp 25-47.

[2] Boyd, J.; Oza, M.N.; Murphy, J.R. *Proc. Natl. Acad. Sci. USA,* **1990**, *87*, 5968.

[3] Olsnes, S.; Pihl, A. in *The Molecular Action of Toxins and Viruses*; Cohen, P. and Van Heynigen, S., eds; Elsevier Biomedical Press: New York, **1982**; pp.52-105.

[4] Lord, J.M.; Roberts, L.M.; Robertus, J.D. *FASEB J.,* **1994**, *8*, 201.
[5] Robertus, J.D.; Monzingo, A.F. in *Protein Toxin Structure;* Parker, M., Eds.; Landes, R. G.: Austin, TX, **1996**; pp. 253-270.
[6] Olsnes, S.; Kozlov, J.V. *Toxicon,* **2001,** *39*, 1723.
[7] Sandvig, K.; Grimmer, S.; Lauvrak, S.U.; Torgersen, M.L.; Skretting, G.; van Deurs, B.; Iversen, T.G. *Histochem. Cell Biol.,* **2002**, *117*, 131.
[8] Endo, Y.; Tsurugi, K. *J. Biol. Chem.,* **1987**, *262*, 8128.
[9] Endo, Y.; Chan, Y.L.; Lin, A.; Tsurugi, K.; Wool, I.G. *J. Biol. Chem.,* **1988**, *263*, 7917.
[10] Olsnes, S.; Fernandez-Puentes, C.; Carrasco, L.; Vasquez, D. *Eur. J. Biochem.,* **1975**, *60*, 281.
[11] Ready, M.; Bird, S.; Rothe, G.; Robertus, J.D. *Biochem. Biophys. Acta,* **1983**, *740*, 19.
[12] Ready, M.P.; Kim, Y.S.; Robertus, J.D. *Proteins,* **1991**, *10*, 270.
[13] Barbieri, L.; Battelli, M.G.; Stirpe, F. *Biochim. Biophys. Acta*, **1993,** *1154*, 237.
[14] Ready, M.P.; Brown, D.T.; Robertus, J.D. *Proc. Nat. Acad. Sci. USA,* **1986**, *83*, 5053.
[15] Lodge, J.K.; Kaniewski, W.K.; Tumer, N.E. *Proc. Natl. Acad. Sci. USA,* **1993**, *90*, 7089.
[16] Fodstad, O.; Olsnes, S.; Pihl, A. *Br. J. Cancer,* **1976**, *34*, 418.
[17] Svinth, M.; Steighardt, J.; Hernandez, R.; Suh, J.; Kelly, K.; Day, P.; Lord, M.; Girbes, T.; Robertus, J.D. *Biochem. Biophys. Res. Comm*., **1998,** *249*, 637.
[18] Montfort, W.; Villafranca, J.E.; Monzingo, A.F.; Ernst, S.R.; Katzin, B.; Rutenber, E.; Nuyhen, H.X.; Hamlin, R.; Robertus, J.D. *J. Biol. Chem.,* **1987**, *262*, 5398.
[19] Rutenber, E.; Katzin, B.J.; Collins, E.J.; Mlsna, D.; Ernst, S.E.; Ready, M.P.; Robertus, J.D. *Proteins,* **1991**, *10*, 240.
[20] Katzin, B.J.; Collins, E.J.; Robertus, J.D. *Proteins,* **1991**, *10*, 251.
[21] Rutenber, E.; Robertus, J.D. *Proteins,* **1991**, *10***,** 260.
[22] Mlsna, D.; Monzingo, A.F.; Katzin, B.J.; Ernst, S.; Robertus, J.D. *Prot. Sci.,* **1993**, *2*, 429.
[23] Weston, S. A.; Tucker, A.D.; Thatcher, D.R.; Derbyshire, D.J.; Pauptit, R.A. *J. Mol. Biol.,* **1994**, *244*, 410.
[24] Monzingo, A.F.; Robertus, J.D. *J. Mol. Biol.,* **1992**, *227*, 1136.
[25] Schlossman, D.; Withers, D.; Welsh, P.; Alexander, A.; Robertus, J.D.; Frankel, A. *Mol. Cell Biol.,* **1989**, *9*, 5012.
[26] Frankel, A.; Welsh, P.; Richardson, J.; Robertus, J.D. *Mol. Cell. Biol.*, **1990**, *10*, 6257.
[27] Kim, Y.S.; Robertus, J.D. *Protein Engineering,* **1992**, *5*, 775.
[28] Chen, X.Y., Link, T.M.; Schramm, V.L. *Biochemistry*, **1998**, *37*, 11605.
[29] Tanaka, K.S.E.; Chen, X.-Y.; Ichikawa, Y.; Tyler, P.C.; Furneaux, R.H.; Schramm, V.L. *Biochemistry,* **2001**, *40*, 6845.
[30] Villafranca, J.E.; Robertus, J.D. *J. Biol. Chem.,* **1981**, *256*, 554.
[31] Rutenber, E.; Ready, M.; Robertus, J. D. *Nature,* **1987**, *326*, 624.
[32] Rich, V. *New Scientist*, **1992**, *135,* 8.
[33] De Fiebre, C. *Minneapolis Star-Tribune*, **1995**, March 1, 1B.
[34] Wright, R. *Los Angeles Times*, **1995**, Sept. 6, A1.
[35] Loyd, A.; Fletcher, M. *London Times,* **2001**, November 16, Overseas Section.
[36] Hesselberth, J.R.; Miller, D.; Robertus, J.; Ellington, A.D. *J. Biol. Chem.,* **2000**, *275*, 4937.
[37] Yan, X.; Hollis, T.; Svinth, M.; Day, P.; Monzingo, A.F.; Milne, G.W.A.; Robertus, J.D. *J. Mol. Biol*., **1997**, *266*, 1043.
[38] Yan, X.; Day, P.; Hollis, T.; Monzingo, A.F.; Schelp, E.; Robertus, J.D.; Wang, S.; Milne, G.W. *Proteins,* **1998**, *31*, 33.
[39] Miller, D.J.; Ravikumar, K.; Shen, H.; Suh, J.K.; Kerwin, S.M.; Robertus, J.D. *J. Med. Chem.*, **2002**, *45*, 90.
[40] Brigotti, M.; Rizzi, S.; Carnicelli, D.; Montanaro, L.; Sperti, S. *Life Sci.,* **2000**, *68*, 331.
[41] Fraser, M.E.; Chernaia, M.M.; Kozlov, Y.V.; James, M. N. *Nat. Struct. Biol*., **1994**, *1*, 59.
[42] Girbés, T.; Citores, L.; Iglesias, R.; Ferreras, J.M.; Muñoz, R.; Rojo, M.A.; Arias, F.J.; García, J.R.; Méndez, E.; Calonge, M.; Ebulin, l. *J. Biol. Chem.*, **1993**, *268*, 18195.
[43] Pascal, J.M.; Day, P.J.; Monzingo, A.F.; Ernst, S.R.; Robertus, J.D.; Iglesias, R.; Perez, Y.; Ferreras, J.M.; Citores, L.; Girbes, T. *Proteins: Struct., Funct., Genet*., **2001**, *43*, 319.
[44] Monzingo, A.F.; Collins, E.J.; Ernst, S.R.; Irvin, J.D.; Robertus, J.D. *J. Mol. Biol.,* **1993,** *233*, 705.
[45] Ren, J.; Wang, Y.; Dong, Y.; Stuart, D.I. *Structure,* **1994**, *2*, 7.
[46] Huang, Q.; Liu, S.; Tang, Y.; Jin, S.; Wang, Y. *Biochem J.,* **1995**, *309*, 285.
[47] Kurinov, I.V.; Myers, D.E.; Irvin, J.D.; Uckun, F.M. *Protein Sci.,* **1999**, *8*, 1765.
[48] Gu, Y. J.; Xia, Z. X. *Proteins,* **2000**, *39*, 37.
[49] Xiong, J.P.; Xia, Z.X.; Wang, Y. *Nat. Struct. Biol*., **1994**, *1*, 695.
[50] Kurinov, I.V.; Rajamohan, F.; Venkatachalam, T.K.; Uckun, F.M. *Protein Sci*., **1999**, *8*, 2399.
[51] Husain, J.; Tickle, I.J.; Wood, S.P. *FEBS Lett,* **1994,** *342*, 154.
[52] Hosur, M.V.; Nair, B.; Satyamurthy, P.; Misquith, S.; Surolia, A.; Kannan, K.K *J. Mol. Biol.,* **1995,** *250*, 368.
[53] Tahirov, T.H.; Lu, T.H.; Liaw, Y.C.; Chen, Y.L.; Lin, J.Y. *J. Mol. Biol.,* **1995**, *250*, 354.
[54] Day, P.J.; Ernst, S.R.; Frankel, A.E.; Monzingo, A.F.; Pascal, J.M.; Molina-Svinth, M.C.; Robertus, J.D. *Biochemistry,* **1996**, *35*, 11098.
[55] Krauspenhaar, R.; Eschenburg, S.; Perbandt, M.; Kornilov, V.; Konareva, N.; Mikailova, I.; Stoeva, S.; Wacker, R.; Maier, T.; Singh, T.; Mikhailov, A.; Voelter, W.; Betzel, C. *Biochem. Biophys. Res. Comm*., **1999,** *257*, 418.
[56] Zhu, G.; Huang, Q.; Qian, M.; Tang, Y. *Biochim. Biophys. Acta,* **2001**,1548, *152*.
[57] Yuan, Y.-R.; He, Y.-N.; Xiong, J.-P.; Xia, Z.-X. *Acta Crystallogr., Sect. D,* **1999**, *55*, 1144.
[58] Day, P.J.; Lord, J.M.; Roberts, L.M. *Eur. J. Biochem.*, **1998**, *258*, 540.
[59] Rajamohan, F.; Venkatachalam, T.K.; Irvin, J.D.; Uckun, F.M. *Biochem. Biophys. Res. Comm*., **1999**, *260*, 453.
[60] Rajamohan, F.; Kurinov, I.V.; Venkatachalam, T.K.; Uckun, F.M. *Biochem. Biophys. Res. Comm.,* **1999**, *263*, 419.
[61] Smyth, D.G. *Methods in Enzymology,* **1967**, *11*, 214.
[62] Barlow, P.N.; Appleyard, R.J.; Wilson, J.O.; Evans, J.N. *Biochemistry,* **1989,** *28*, 7985.
[63] Anderson, K.S.; Johnson, K.A. *Chem. Rev.,* **1990,** *90*. 1131.
[64] Ago, H.; Kataoka, J.; Tsuge, H.; Habuka, N.; Inagaki, E.; Noma, M.; Miyano, M. *Eur. J. Biochem*., **1994,** *225*, 369.
[65] Wang, Y.-X.; Neamati, N.; Jacob, J.; Palmer, I.; Stahl, S.J.; Kaufman, J.D.; Huang, P.L.; Huang, P.L.; Winslow, H.E.; Pommier, Y.; Wingfield, P.T.; Lee-Huang, S.; Bax, A.; Torchia, *Cell,* **1999**, *99*, 433.
[66] Zhou, K.; Fu, Z.; Chen, M.; Lin, Y.; Pan, K. *Proteins: Struct., Funct., Genet.,* **1994**, *19*, 4.
[67] Gawlak, S.L.; Neubauer, M.; Klei, H. E.; Chang, C. Y.; Einspahr, H. M.; Siegall, C. B. *Biochemistry,* **1997**, *36*, 3095.
[68] Savino, C.; Federici, L.; Ippoliti, R.; Lendaro, E.; Tsernoglou, D. *FEBS Lett.,* **2000**, *470*, 239.
[69] Valbonesi, P.; Barbieri, L.; Bolognesi, A.; Bonora, E.; Polito, L.; Stirpe, F. *Life Sciences,* **1999**, *14*, 1485.